Experimental Assessment of Rotor Superconducting Stack Demagnetization in LN_2 Environment

Anis Smara[1], Nikolay Mineev[1,2], Vicente Climente-Alarcon[1], Anup Patel[1], Algirdas Baskys[1,3], Bartek A. Glowacki[1,4] and Thomas Reis[5]

[1] Department of Materials Science and Metallurgy, University of Cambridge, CB3 0FS, Cambridge, UK
[2] Bruker BioSpin AG, Industriestrasse 26, 8117, Faellanden, Switzerland
[3] CERN - Conseil Européen pour la Recherche Nucléaire, 1217 Meyrin, Switzerland
[4] Institute of Power Engineering, 01-330 Warsaw, Poland
[5] Oswald Elektromotoren GmbH, 63897 Miltenberg, Germany

E-mail: vc363@cam.ac.uk

Received: 06 March 2019
Accepted for publication xxxxxx
Published xxxxxx

Abstract

Stacks of high temperature superconducting tape have proved to trap in laboratory conditions levels of magnetic flux density one order of magnitude above actual state-of-the-art permanent magnets. Their simple manufacturing, high mechanical properties and intrinsic resistance to sudden quench greatly facilitate their utilization in industrial applications, amongst them, as source of magnetic flux density in the rotor of electrical machines. For this to happen, the currents induced in the superconducting layers of the stack must not be disturbed during operation. This work studies in experimental conditions the demagnetization of a stack rotating in the airgap of an electrical motor under slot and winding induced cross-field components, whose values are estimated via conventional 2-D finite element analysis. The results are congruent with previous laboratory studies and show small long-term demagnetization rates that may allow operation for time spans longer than initially established.

Keywords: superconducting motor, trapped-field magnet, high temperature superconductor, demagnetization, liquid nitrogen

1. Introduction

Trapped-field magnets composed of layers of high temperature superconductor (HTS) constitute a promising solution to increase the magnetic flux density available in equipments such as rotating electrical machines [1].

For this task the superconducting stacks are a suitable choice, since they can provide a simpler arrangement with either no need of current leads, compared to field windings [2] or cages [3] that increase the complexity in an element, the rotor, already subjected to important mechanical and thermal requierements. Furthermore, stacks feature a high mechanical resistance [4] due to the superalloy substrate upon which this textured HTS is deposited and bending, necessary for instance to follow the curvature of the rotor, doesn't sharply alter their electrical characteristics [5]. Additionally, the layered structure of the stacks evens out any point defect in the superconductor, averaging its behaviour [6] and it is intrinsically resistant to sudden quench, being the loss of magnetization progressive and noticeable in the output in the machine.

Nonetheless, the currents trapped in the stacks must be induced prior and kept undisturbed during the operation of the machine. Field cooling or current pulses are strategies for magnetizing the stacks, for instance, using the stator coils. However, since variations of magnetic flux density affect them [6] maintaining those trapped currents during operation of the machine is a more complicated matter. Normal variations cause heating due to hysteresis [7] and tangential variations (cross-fields) induce an electrical field that yields a dynamic resistance, rapidly dissipating the trapped currents. The laminated structure of the stacks provides a high aspect ratio, which increases the Lorentz force needed for de-pinning the magnetic vortices and hence the resistance to demagnetization is greater than in bulks [8]; however, it has been reported from laboratory testing that cross fields in the same order the magnitude than the trapped field in each layer demagnetize the stack in just a few hundred cycles [9].

In the airgap of an electrical motor there will be always a plethora of harmonics caused by the differences of permeability of the magnetic circuit (slot harmonics) [10] and the discrete distribution of the stator coils (winding harmonics) [11]. These harmonics are tackled in conventional machines by covering the rotor with a conductive sleeve or simply by burying the magnetically active elements inside the rotor iron [12, 13]. In either case drawbacks exist, the conductive sleeve warms up during operation, which would increase the thermal load that must be dissipated through the stacks by the rotor [14] and the internal configuration adds leakage paths around them that limit the flux linkage value in the airgap [12, 13]. Only recently specific rotor lay-outs to be used with superconducting stacks have been proposed to tackle those conflicting requirements [15]. Other approaches consists of smoothing the airgap from the stator side, either by using an air winding [16], by closing the stator slots by magnetic wedges [17] or prolonging the teeth tips themselves. This later strategy was the one implemented in the design of the machine employed in this experiment.

Although several publications have appeared recently addressing the question of the demagnetization of stacks in laboratory conditions, and even some solutions have been described [8], there seems to be a lack of sufficent data on how a superconducting stack will behave in the airgap of an electrical machine. Thus, this work is aimed at tackling this question by experimentally testing at liquid nitrogen temperature a trapped-field magnet attached to the moving rotor of an electrical machine. After pulse magnetization, the effect of the slot harmonics and increasing stator currents in the demagnetization process of the stack is evaluated. The complex conditions in the airgap of the machine are estimated by conventional 2D finite element analysis. The results show that the drawbacks of using stacks in an electrical machine are not so acute as earlier works in laboratory conditions suggested.

For this purpose the remaining of the paper is organized as follows: Section 2 briefly describes the finite element (FE) model used to estimate the magnetic environment the stacks face during the experiments. Section 3 provides an overview of the methodolgy developed, Section 4 presents the results, and Section 5, the conclusions.

2. Computation of the harmonic content

The intrincate electromagnetic environment the stacks are going to experience during the tests is assessed by a conventional 2D finite element approach that processes the cross section of the motor, as it is commonly carried out in the study of radial electrical machines [11, 18].

2.1 Finite Element model

The magnetic vector potential distribution perpendicular to the section of the machine A is calculated by the Finite Element method [18] using (1):

$$-\nabla \cdot \left(\frac{1}{\mu}\nabla A\right) + \sigma \frac{\partial A}{\partial t} = k \tag{1}$$

where, μ is the magnetic permeability of the material, σ its electrical conductivity and k accounts for the current density in the stator winding areas and stack, and zero elsewhere. From (1) the magnetic flux density is computed as (2):

$$\boldsymbol{B} = \nabla \times \boldsymbol{A} \tag{2}$$

The material for the stator and rotor yoke is silicon iron M270-35A with a saturation level of around 1.7 T, whereas for the rest of the machine the regions are considered to have the characteristics of air, as it is customary in this kind of computations.

Similarly, the currents imposed to the stator coils have been shared as a current density established perpendicularly to the section of the machine in the corresponding domains. Against the usual procedure of imposing a remanent magnetic flux density to simulate the permanent magnets, in this work it was prefered to also inject a current of the same magnitude and opposing sign on each half of the stack. This better approximates the triangular profile of the flux trapped, closer to what can be observed in experimental measurements [19], although the reaction of the supercurrents flowing in the stack to the variations of the magnetic flux density caused by the slot and winding harmonics cannot be reproduced in this way.

2.2 Motor characteristics

The demagnetization experiments have been carried out in an actual electric motor having the characteristics shown in Table I. The double-layer fractional slot non-overlappig winding of the stator design encompasses closed teeth, which,

as said, limit the slot harmonics and therefore enhance the survability of the stack. Copper coils are wounded around each teeth and have been numbered according to Fig. 1. The robust design of the coils permitts their use also as pulse magnetization elements for the stack, although at lower currents, by means of an existing capacitor bank. The tooth coil design allows other coils being used to create different magnetic flux patterns inside the machine or retrieve, employed as test coils, the variations of its distribution in the airgap with little coupling among them. The rotor features a circular shaped surface and the stack is arranged accordingly on its external face, acting thus as a surface mounted permanent magnet.

TABLE I
MOTOR CHARACTERISTICS

Stator external diameter	236 mm
Stator internal diameter	120 mm
Airgap length	2 mm
Stack height	1 mm
Rotor yoke external diameter	114 mm
Rotor yoke internal diameter	36 mm
Machine length	160 mm
Number of pole pairs	(4)
Stator turns per coil	21.5
Demagnetizing currents	3.5-20 A DC
Simulated current density in the stacks	$1.31 \cdot 10^7$ A/m^2

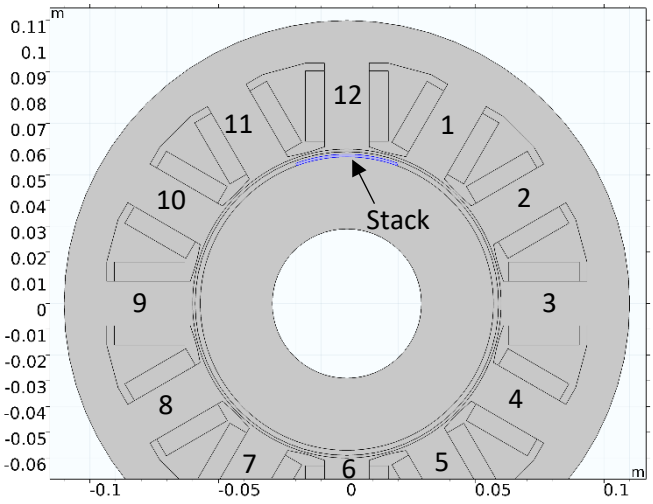

Fig. 1. Cross section of the machine with the teeth/coils numbered. The stack positioned on the rotor´s surface is marked in blue.

3. Experimental procedure

This section describes the process followed to evaluate the demagnetization rate of a stack of superconductive tape in the airgap of an electrical machine. It is divided in three points. The first one presents the experimental setup, the second one the magnetization procedure followed to induce the currents in the stack and the last one the arrangements to obtain its demagnetization profile in a controlled way.

3.1 Experimental setup

The experimental setup consist of a commercial motor supplied by Oswald Elektromotoren Gmbh installed in a thermal insulated bucket that is filled with liquid nitrogen. A clearance of 3 mm between stator and rotor (see Table I) permitts testing different trapped-field magnet arrangements of up to 1 mm of height, supported by a 1 mm G10 sleeve. A speed-controlled DC motor coupled to the shaft and fitted on the setup above the surface level of the liquid nitrogen provides a variable turning rate for the rotor (see Fig. 2).

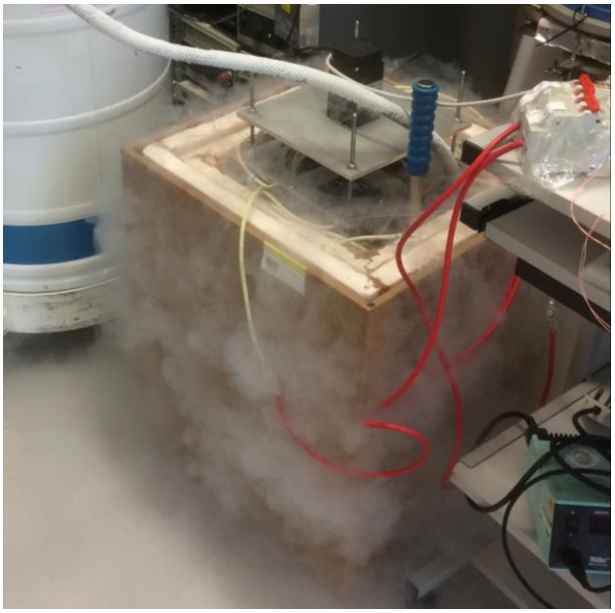

Fig. 2. The setup during operation. Only the DC motor is visible above the insulated bucket.

For this experiment, the stacks consist of 9 layers of AMSC (RE)BCO tape [6], cut to a width of 41 mm, featuring a critical current of 391 A/cm-width at 77 K and self field, and an engineering current of $4.49 \cdot 10^8$ A/m^2. With those dimensions, each layer of AMSC tape can trap 22 mT at 77 K as measured in a Hall scan probe, which provides a theoretical total of 0.2 T. Alternating with the tape, NiFe 50-50 layers with a thickness of 20 μm were added to favour magnetization, but no improvement was observed, maybe caused by the variability inherent to the magnetization process. No soldering was used, being kept the shape of the stack instead by two strips of Kapton tape and the slight compression provided by the rotor's outer sleeve. Due to this arrangement, all the layers are assumed to be surrounded by liquid nitrogen and hence anchored at 77 K, which may improve the magnetization procedure, according to [20].

The diameter of the rotor yields a bending radius for the stacks of 57 mm, which is easily followed by the tape, as it is proved by the recovery of a flat shape after being extracted from the rotor without affecting its electrical characteristics.

3.2 Pulse magnetization

Field cooling and pulse magnetization were evaluated as possible strategies to induce a significant current density in the stacks prior to rotation. The first one was discarded due to the necessity of circulating high currents through the stator during the cooling process of the motor, which would increase the liquid nitrogen consumption. A capacitor bank was used instead [19] connected to coil 12 (see Fig. 1), although charged at a lower voltage in order to save the coil from high stresses during the repeated pulse trains.

With the aim of increasing the flux trapped inside the stack, following [5] an iteratively magnetizing pulsed field method with reduced amplitude (IMRA) was carried out. Ranging from 50 V to 5 V, decrements of 5 V after each pulse were applied with the objective of firstly magnetizing the central part of the stack and then proceeding accordingly to the edges. A period of 30 s was left for flux relaxation and capacitor bank charging in-between the pulses. The level of magnetization attained is assessed by comparing the experimental measurements to the simulations carried out by FE in the results section.

3.3 Demagnetization

In order to perform the controlled demagnetization three other coils from the stator windings were connected to a DC source. Current circulating in coils 3 and 9 produces a flux mostly normal in the airgap, whereas an increase in the tangential component is expected by alternatively feeding the adjacent coils 9 and 10 changing the state of the switches shown in Fig. 2. The rotation of the stack in the airgap provides the flux variation. Values between 3.5 and 20 A for this circuit are available using this power source, although the control is limited above 17 A.

The evolution of the trapped flux in the stack is assessed by measuring the back-emf induced in the coils 5 and 7. A Yokogawa DL-850E oscilloscope-recorder is attached to the first one, number 5, providing a back-*emf* waveform spanning the full experiment. Sampling rates of 10-20 ksamples/second have been used for this purpose to provide a good depiction of the peaks to be observed.

Finally, an estimation of the normal and tangential components of the magnetic flux density that the stacks experience obtained by FE simulation of the conventional motor populate Table II.

TABLE II
NORMAL AND CROSS-FIELD IN THE STACK IN MT

Coil current	Coils 9-3		Coils 9-10	
	ΔB_{norm}	ΔB_{tan}	ΔB_{norm}	ΔB_{tan}
3.5 A	60	8	66	12
7 A	120	18	130	25
13 A	130	36	240	48

Contrary to what was initialy intended, the use of the adjacent Coils 9-10 also increases the normal variation of the magnetic flux density falling on the stack since no smearing across the full rotor iron and through the stator iron bridges takes place in that case due to the small distance between source and sink of flux.

4. Results

This work presents the results of two experiments conducted on the setup introduced in the previous point. The stages followed in both experiments were cooling, pulsed magnetization, rotation and demagnetization by feeding the stator coils. The first one used coils 3-9 to provide a mostly-normal magnetic flux density on the stack and the second one employing coils 9-10, in order to increase the tangential component.

4.1 Pulse magnetization

Some measurements were carried out on the magnetization leads using a 100 A/ 60 mV shunt. The current waveform recorded during a 40 V pulse is shown in Fig. 3 comprising two lobes, lasting 10 ms and peaking at 280 A.

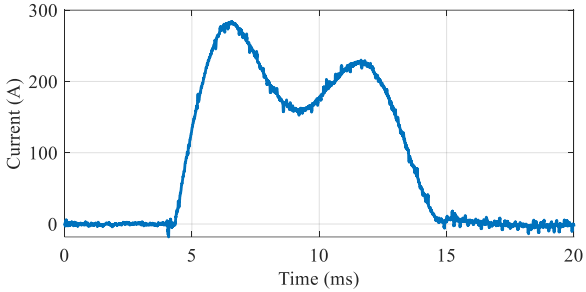

Fig. 3. Current profile during a pulse for the capacitor bank charged to 40 V.

4.2 Rotation

The waveform measured in coil 5 once rotation commences is presented in Fig. 4 showing the voltage induced by the magnetized stack in that tooth. Due to the control of the DC motor turning the rotor, the speed stabilizes around 650 rpm, according to the peak's period, and hence the maximum

voltage amplitude oscillations appreciated in Fig. 4 are attributed to flux creep, since no relaxation period was carried out. Nevertheless, this oscillation is damped in less than 30 s and afterwards the induced *emf* profile remains flat, a sign that the variation of magnetic permeability the stator teeth cause does not affect the stacks. The characteristics of this oscillation are almost identical for both experiments, corresponding to the evolution of a second order underdamped system with time constant of 0.42 s and damping factor of $4 \cdot 10^{-2}$.

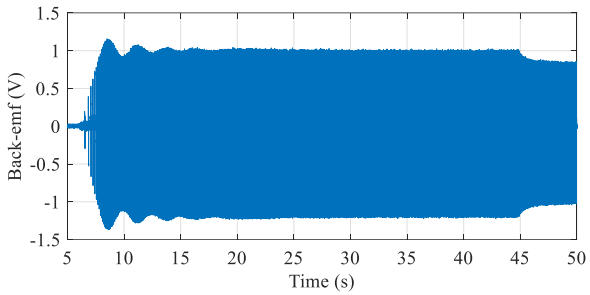

Fig. 4. Evolution of the induced voltage as the rotor is spinned during the first experiment The initial perturbation due to flux creep is fully damped in less than 30 s. At 45 s current is turned on in coils 3-9(see Fig. 6).

Fig. 5 zooms-in into the voltage waveform induced by the stacks for coil 5 during a rotation cycle after flux creep. The results from both experiments are presented along the simulated ones obtained by the model presented in Section 2.

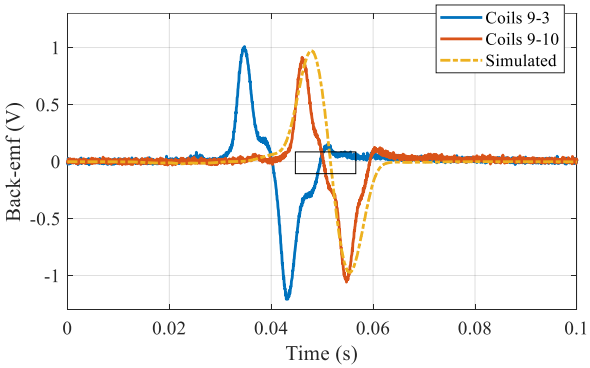

Fig. 5. Waveform comprising the induced voltage in coil 5 by the stack during one rotation for experimental and simulated results. The rectangle represents the approximate size of the stack centered at the zero crossing of the second experiment, using coils 9-10 (see Fig. 1).

Each pulse is composed by two lobes, a positive and a negative one, corresponding to the ascending and descending flanks of the magnetic flux density produced by the trapped currents in the stack, as it passes in front of the tooth. Some damped oscillation or "ringing" appears before and after the main pulsation, related to the saturation of the iron bridges closing the teeth (see Fig. 1). Both experimental waveforms differ in their maximum amplitude by 10 %, a consequence of the limitations of the magnetization method employed. The simulated one was obtained dividing the stack in two and circulating a current of $1.31 \cdot 10^7$ A/m^2 with opposite sign perpendicular to each half. The magnetic flux density yielded on the external surface of the stack by this procedure has triangular shape and peaks at 100 mT, which means that the superconductor is understaturated. The morphology of the magnetic circuit, featuring iron bridges between the teeth, suggest that the flux preferentially penetrates from the sides of the stack, acting on all the superconducting layers in some degree and therefore, this level of trapped flux is shared between all of them. The cross field variations on the stack are estimated by the same method to less than 1 mT during rotation, and cause no demagnetization (Fig. 4). Normal variations are somewhat higher, around 4 mT, but their effect in the heating of the trapped-field magnet cannot be appreciated by this experimental procedure, since the whole motor is immersed in liquid nitrogen.

4.2 Demagnetization

In this point the results concerning the reduction of the magnetic flux density trapped in the stack due to the currents circulating in the stator during both experiments are presented. Fig. 6 depicts the evolution of the peak back-electromotive force induced in the coil 5 by the stack. The first seconds correspond to the rotor just after pulse magnetization and prior to movement, and hence no peaks are detected by the filtering algorithm. Once the rotor is moved by the external DC motor, the peak value of the back-*emf* leaves the oscillatory period and stabilizes, which corresponds to the envolope of the signal shown in Fig. 4. At that point, currents in the stator are established and maintained for at least a minute. Their effect is immediately appreciated as a sharp decline of the back-*emf* –and hence the currents in the stack– followed by a slower decay, well in agreement with the results presented in [9]. However, in this experiments the stack is withstanding more than 10 cycles per second (equivalent to 650 rpm), which is one order of magnitude further than in that work, although the perturbation waveform differs.

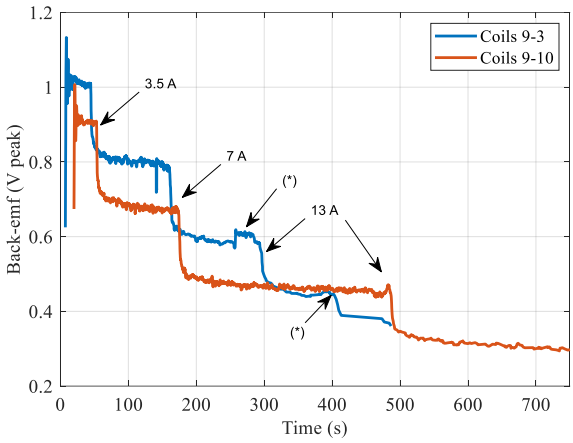

Fig. 6. Decreasing peak back-emf values during both experiments.

The reduction of back-*emf* up to 10 seconds after increasing the current circulating either by coils 9-3 or 9-10 is shown in Table III. The greater tangential component of generated the coils 9-10 (see Table II) is congruent with a higher loss of induced voltage. Furthermore, as a general rule, variations of flux below half the amount trapped in the stack don't induce a rapid loss of magnetization. In such cases, this phenomenon is gradual and damped with increased amplitude of the cross-field.

TABLE III
REDUCTION IN BACK-EMF AFTER 10 S

Coil current	Coils 9-3		Coils 9-10	
	ΔV	%	ΔV	%
3.5 A	0.18	18	0.23	24
7 A	0.16	20	0.19	28
13 A	0.1	17	0.1	22

The long term trend after each reduction in back-*emf* has been evaluated by assuming a linear evolution and fitting the corresponding polynomial to the last segments of signal after each increase in stator current. The results are presented in Table IV. Higher values are observed for the experiment using coils 3-9, however, this may be caused by the fact that the time span evaluated is usually shorter. In any case, these slopes suggest that, under these conditions, periods of operation lasting thousands of seconds are possible.

TABLE IV
LONG TERM BACK-EMF REDUCTION RATES

Coil current	Coils 9-3 V/s	Coils 9-10 V/s
3.5 A	$-2.3\cdot10^{-4}$	$-1.5\cdot10^{-4}$
7 A	$-9.6\cdot10^{-5}$	$-7.6\cdot10^{-5}$
13 A	$-1.5\cdot10^{-4}$	$-1.3\cdot10^{-4}$

Furthermore, in this magnitude's evolution it is clearly appreciated higher maximum amplitudes of the peaks just before the stator current is increased, marked in Fig. 6 as (*), especially before the 13 A step during the first experiment, using Coils 9-3. In this period the stator was de-energized to allow checking only the influence of the stack in the back-*emf* waveform after some level of demagnetization happened. Conventional FE simulations reproduce this same behaviour, which is related to the altered magnetic flux density distribution in the rotor by feeding the stator coils and not to any recovering of the currents in the stack. The influence is smaller in the case of the second experiment, since in this case coils 9-10 sit in the opposite side of the magnetic circuit in this case and thus little or no smearing of their flux reaches coil 5.

These results offer encouraging prospects for the operation of stacks in synchronous machines, since this performance can be extrapolated to lower temperatures following previous studies in static conditions [21]. Simply by reducing the temperature of the rotor to 50 K the field necessary to fully penetrate the stacks increases around 250%, therefore, either much less susceptibility to demagnetization is expected under those conditions or the cross-field components shown in Table II could be increased accordingly. Moreover, the higher frequencies that these harmonics feature in an actual electrical machine might also lessen this effect [22]. Finally, other stack configurations may be easily arranged in this setup and tested, such as using angle stacks [23] to trading some cross-field components for normal ones.

5. Conclusions

The application of trapped-field magnets as the source of magnetic flux density in electric motors appears to be less problematic than early studies in laboratory conditions suggested. For initial operation, no flux relaxation period in the stack after magnetization seems to be necessary, happening naturally during a few seconds of rotation. Furthermore, the demagnetization profile due to cross-fields in the airgap of an electrical machine featuring variations lower than half the trapped flux value, agree with previous laboratory studies and present an initial rapid reduction, followed by an slow decay, which can be used for motoring during thousands of seconds. Increasing variations of the cross-field have smaller impact in the flux trapped in the stack. The study, however, doesn't reproduce actual conditions for motoring and doesn't take into account the heating of the stacks by the losses induced by the normal magnetic flux density variation.

Acknowledgements

This research is financially supported by the European Union's Horizon 2020 research innovation programme under grant agreement No 7231119 (ASuMED consortium) and also by EPSRC grant EP/P000738/1.

References

[1] Climente-Alarcon V, Patel A, Baskys A, Glowacki B A, 2019 IOP Conf. Ser.: Mater. Sci. Eng.502 012182.

[2] Kong W, Terao Y and Ohsaki H, "Optimal Design of a Superconducting Motor for Electric-drive Aeropropulsion Based on Finite-Element Analysis and Genetic Algorithm," 2018 *J. Phys.: Conf. Ser.* 1054 012082

[3] Nakamura T, Matsumura K, Nishimura T, Nagao K, Yamada Y, Amemiya N, Itoh Y, Terazawa T, Osamura, K, 2011"A high temperature superconducting induction/synchronous motor with a ten-fold improvement in torque density," *Supercond. Sci. Technol.* **24** 015014

[4] Patel A, Baskys A, Mitchell-Williams T, McCaul A, Coniglio W, Hänisch J, Lao M, Glowacki B A, 2018, "A trapped field of 17.7 T in a stack of high temperature superconducting tape," *Supercond. Sci. Technol.*, **31** 9

[5] Shengnan Zou, "Magnetization of High Temperature Superconducting Trapped-Field Magnets," PhD Thesis, KIT Scientific Publishing, 2017. (Available on-line: https://publikationen.bibliothek.kit.edu/1000073152)

[6] Patel A, Baskys A, Hopkins S C, Kalitka V, Molodyk A and Glowacki B A, 2015, "Pulsed-Field Magnetization of Superconducting Tape Stacks for Motor Applications," *IEEE Trans. Appl. Supercond*., **25** 3 5203405

[7] Iwasa Y, Case Studies in Superconducting Magnets, Design and Operational Issues, Second edition, Springer, 2009.

[8] Baghdadi M, Ruiz H S, Fagnard J F, Zhang M, Wang W, and Coombs T A, 2015, "Investigation of Demagnetization in HTS Stacked Tapes Implemented in Electric Machines as a Result of Crossed Magnetic Field*," IEEE Trans. Appl. Supercond.*, **25**, 3, 6602404

[9] A. Campbell, M. Baghdadi, A. Patel, D. Zhou, K. Y. Huang, Y. Shi and T. Coombs, 2017, "Demagnetisation by crossed fields in superconductors," *Supercond. Sci. Technol.*, **30** 3, 034005

[10] Patel A, Climente-Alarcon V, Baskys A, Glowacki B A amd Reis T, "Design considerations for fully superconducting synchronous motors aimed at future electric aircraft," *IEEE 5th International Conference on Electrical Systems for Aircraft, Railroad, Ship Propulsion and Road Vehicles and International Transportation Electrification Conference*, Nottingham, United Kingdom, November 2018

[11] Di Tommaso A O, Genduso F and Miceli R, 2015, "A New Software Tool for Design, Optimization, and Complete Analysis of Rotating Electrical Machines Windings," *IEEE Trans. Mag*. **51** 4, 9401410

[12] Rao J, Ronghai Q, Jimin M and Xu W, "Investigate the influence of magnetic bridge design on mechanical strength and electromagnetic characteristics in high speed IPM machines," *2014 17th International Conference on Electrical Machines and Systems (ICEMS)*, 22-25 Oct. 2014

[13] Pyrhönen J, Tapani, J and Hrabovcova V, Design of Rotating Electrical Machines, Second Edition, Wiley, 2014.

[14] Ahn J, Han C, Kim C and Choi J, 2018, "Rotor Design of High-Speed Permanent Magnet Synchronous Motors Considering Rotor Magnet and Sleeve Materials," *IEEE Trans. Appl. Supercond.*, **28** 3 5201504

[15] Climente-Alarcon V, Smara A, Patel A, Glowacki B, Baskys A. and Reis T, (accepted for presentation), Field Cooling Magnetization and Losses of an Improved Architecture of Trapped-Field Superconducting Rotor for Aircraft Applications, *AIAA Propulsion and Energy Forum and Exposition*, Indianapolis, Indiana, August 2019 (3189332)

[16] Lea T D, Kima J H, Kima D J, Boob C J, and Kim H M, 2015, "Status of the technology development of large scale HTS generators for wind turbine, Progress in Superconductivity and Cryogenics," **17**, 2, pp. 18~24

[17] Han S, Jung J, Lee K W, Lee S B, Nandi S, Kim B and Kang B, 2016, "In-Service Monitoring of Stator-Slot Magnetic Wedge Condition for Induction Motors," *IEEE Trans. Ind. Appl*, **52** 4, Page s: 2900 - 2910

[18] Boldea I and Tutelea L, Electric Machines: steady state, transients and design with Matlab, CRC press, 2010.

[19] Patel A, Hopkins S C, and Glowacki B A, 2013, "Trapped fields up to 2 T in a 12 mm square stack of commercial superconducting tape using pulsed field magnetization," *Supercond. Sci. Technol*, **26** 032001

[20] Patel A, Filar V, Nizhankovskii I, Hopkings S C, Glowacki B A, 2013, "Trapped fields greater than 7 T in a 12 mm square stack of commercial high-temperature superconducting tape", *Appl.Phys.Letts.*, **102,** 102601.

[21] Baskys A, Patel A, Glowacki B A, 2018, "Measurements of crossed-field demagnetisationrate of trapped field magnets at high frequencies and below 77 K", *Supercond. Sci. Technol.*, **31,** 065011

[22] Mitchell-Williams T B, Baskys A, Hopkings S C, Kalitka V, Molodyk A, Glowacki B A, Patel A, 2016, "Uniform trapped fields produced by stacks of HTS coated conductor tape", *Supercond. Sci. Technol.*, **29,** 085008.

[23] Baghdadi M, Ruiz H S, Coombs T A, 2014, "Crossed-magnetic field experiments on stacked second generation superconducting tapes: reduction of the demagnetization effects", *Appl. Phys. Lett*., **104**, 232602.